

Reports

X-Ray Line and Continuum Spectra of Solar Flares from 0.5 to 8.5 Angstroms

Abstract. Two crystal spectrometers aboard the orbiting solar observatory *OSO-4* cover the wavelength ranges 0.5 to 3.9 angstroms and 1.0 to 8.5 angstroms. Within this range, there appear emission lines from hydrogen-like and helium-like states of calcium, sulfur, silicon, magnesium, and aluminum. The Mg XII Lyman- α is present strongly in all x-ray flares. The most intense flares (such as class 3) produce strong Si XIV Lyman- α and often S XVI Lyman- α . Emission, in the form of K α lines of highly ionized states of calcium, iron, aluminum, and silicon is usually present. The continuum from 1 to 10 angstroms always dominates the line emission by more than an order of magnitude. Electron temperatures derived from the slope of the continuum spectrum are in the range of 10^7 to 10^8 °K, considerably higher than theoretical ionization equilibrium temperatures.

We present some early results from an x-ray spectrometer aboard the NASA orbiting solar observatory *OSO-4* spacecraft. The spectrometer experiment is designed to record spectra of solar flares at wavelengths below 8.5 Å. Since its launch in October 1967, data have been obtained for a number of solar flares ranging in size from small subflares to large flares of class 3b (3 bright).

The *OSO-4* instrument consists of two Bragg crystal spectrometers which lie

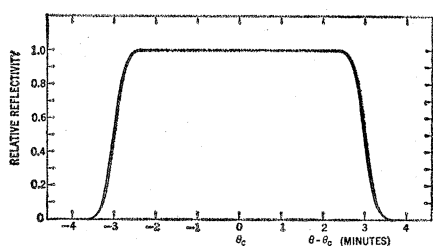


Fig. 1. Ideal reflectivity of the bent crystal. The total angle of bend is 6 arc min.

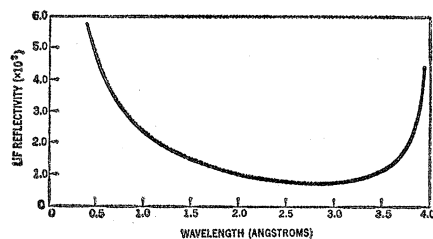


Fig. 2. Integrated reflectivity of the LiF crystal as calculated from the kinematic theory (1, 2).

one above the other on a common axis of rotation and are driven by the same stepping motor. According to Bragg's law:

$$n\lambda = 2d \sin \theta$$

where n is the order of diffraction ($n = 1$ in this experiment), λ is the wavelength of the radiation diffracted, d is the atomic plane spacing of the crystal, and θ is the angle between the incident radiation and the atomic planes of the crystal. One of the spectrometers has a LiF ($2d = 4.03$ Å) crystal; the other uses an EDDT (ethylenediamine- d -tartrate; $2d = 8.81$ Å) crystal. The spectral ranges covered are 0.6 to 3.9 Å and 1.4 to 8.5 Å, respectively.

A filter over the entrance aperture reduces heating within the instrument enclosure and also reflects ultraviolet radiation to which the instrument might respond. The filter is composed of 0.00025-inch thick Mylar ($C_{10}H_8O_4$; area density $\rho_X = 0.84$ mg cm^{-2}) on which 2000 Å of aluminum (1000 Å on each side) has been evaporated. The detectors in each spectrometer are argon-filled ($\rho_X = 2.6$ mg cm^{-2}) Geiger counters. The quench agent is 1 percent bromine, and the windows are mica ($\rho_X = 1.5$ mg cm^{-2}). The cosmic-ray background is about 4 count/sec.

Bragg's law describes the condition under which x-rays are reflected from a crystal at maximum efficiency. However, some reflection occurs at angles which

depart slightly from the Bragg angle. Thus monochromatic radiation is spread over a small range of angles upon reflection from the crystal. The intensity-versus-angle relation is called the rocking curve of the crystal. The FWHM (full width at half maximum) of the rocking curve is about 2 arc min for the EDDT crystal and about 20 arc min for the LiF crystal used in this spectrometer. A stepping motor moves the crystal in steps of angle $\Delta\theta = 6$ arc min. Since x-ray linewidths from a flat crystal can be expected to be somewhat narrower than this, there would be a definite possibility of missing the peak of a line (of stepping over a line). For this reason, the EDDT analyzing crystal was slightly bent to give a rocking curve similar to the one shown in Fig. 1. With a crystal bent in this fashion, stepping over a line is not possible, and analysis of recorded line strengths is simplified; yet wavelengths can still be measured to less than 0.005 Å. However, since an x-ray source may be anywhere on the solar disk, not necessarily where the instrument is pointing, our maximum absolute error is about 0.03 Å for wavelength determination, before correction for source displacement.

In order to correct the data to photon flux, the transmission of the filter T , the reflectivity of the crystal R , and the photon efficiency of the Geiger counter ϵ must be determined. These parameters, together with the effective aperture area A , determine the relation be-

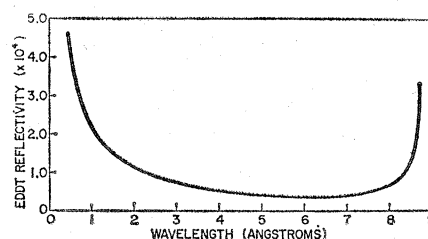


Fig. 3. Integrated reflectivity of the EDDT crystal as calculated from the kinematic theory (1, 2).

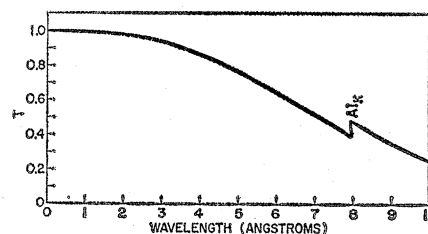


Fig. 4. Transmission of the aluminum-coated Mylar filter.

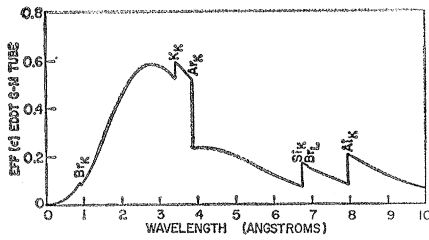


Fig. 5. Quantum efficiency of the Geiger-Mueller detector of the EDDT spectrometer. (Efficiency of the detector of the LiF spectrometer is similar.)

tween the measured counting rate C and the incident photon flux I :

$$I = C/ART\epsilon \quad (1)$$

where R , T , and ϵ are functions of λ , and R may be calculated approximately by the kinematic theory of the diffraction of crystals (I). The results of such calculations for crystals of LiF and EDDT are shown in Figs. 2 and 3, respectively. Values for T and ϵ may be calculated from

$$T = \exp [-(\mu_m \rho X)_{\text{Mylar}} - (\mu_m \rho X)_{\text{Al}}] \quad (2)$$

$$\epsilon = \exp [-(\mu_m \rho X)_{\text{mica}}] \times \{ 1 - \exp [-(\mu_m \rho X)_{\text{Ar}} - (\mu_m \rho X)_{\text{Br}}] \} \quad (3)$$

where ρX and μ_m are the appropriate area densities and mass absorption co-

efficients, respectively. From mass absorption coefficients determined by Henke (2), T and ϵ have been calculated as a function of wavelength. The results are shown in Figs. 4 and 5. Application of these results to raw data does not remove the discontinuities which appear at absorption edges. In fact, the correction is too great in some cases, and a step decrease across the absorption edge becomes a step increase. This casts doubt upon the validity of the calculated values of T , R , and ϵ even at wavelengths somewhat removed from the absorption edges. We believe that, over most of the wavelength range, the system constants permit calculation of the flux values to within 25 percent; at the very shortest wavelengths and right at the edges, the error may reach a factor of 3.

Many flares have been recorded, but analysis of the data has thus far been by hand, and not many orbits have been reduced. Of the solar events we have studied, we chose three for discussion.

The first of these, a class 1b flare, occurred on 26 October 1967, at about 0617 U.T. The raw data are plotted from the LiF and EDDT spectrometers (Figs. 6 and 7). The duration of the flare was too short to get one complete

spectral scan (which takes approximately 13 minutes). The edges which appear at 3.9 and 7.9 Å are caused by the argon in the detectors and the aluminum in the mica windows and filter. The feature in Fig. 6 at about 3.2 Å has been identified as K line radiation from Ca XVII and Ca XVIII at 3.22 Å plus resonance radiation from Ca XIX at 3.19 Å. The resonance line and the K lines are clearly resolved in the spectrum taken between 21780 U.T. and 22625 U.T. In Fig. 7, only the most dominant lines have been labeled, but it is clear from the data that lines at 7.99, 8.14, 8.22, and 8.33 Å are present. These may be identified as K lines of Al X, Al VIII, Al VII, and Al V. The additional line at 8.06 Å may be a blend of Fe XXIV $2s-4p$ and the K line of Al IX. The rising continuum at shorter wavelengths is caused by increasing reflectivity of the crystal toward grazing incidence. Folded into the spectral scans (Figs. 6 and 7) is the development and decay of the flare with time, so little can be said quantitatively about relative spectral intensities at any instant of time.

If we examine the ratio of the Ca XIX line to the Ca XVII and Ca XVIII lines in Fig. 6, we find that in the earlier

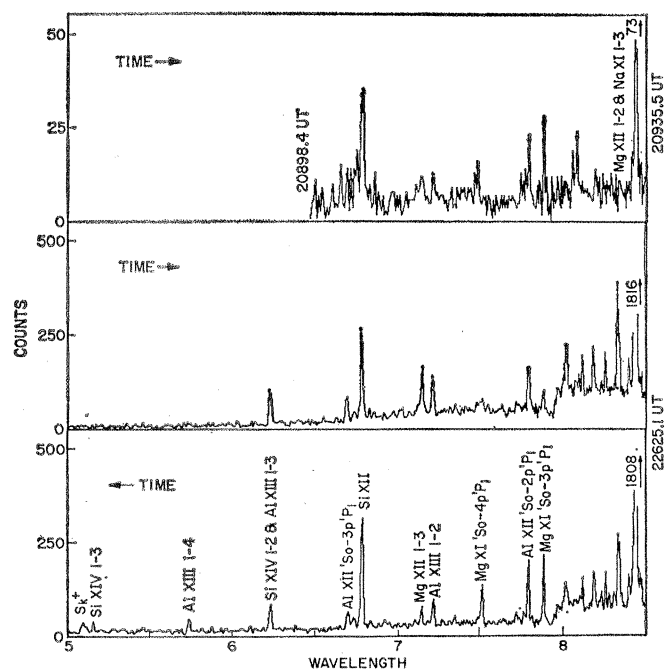
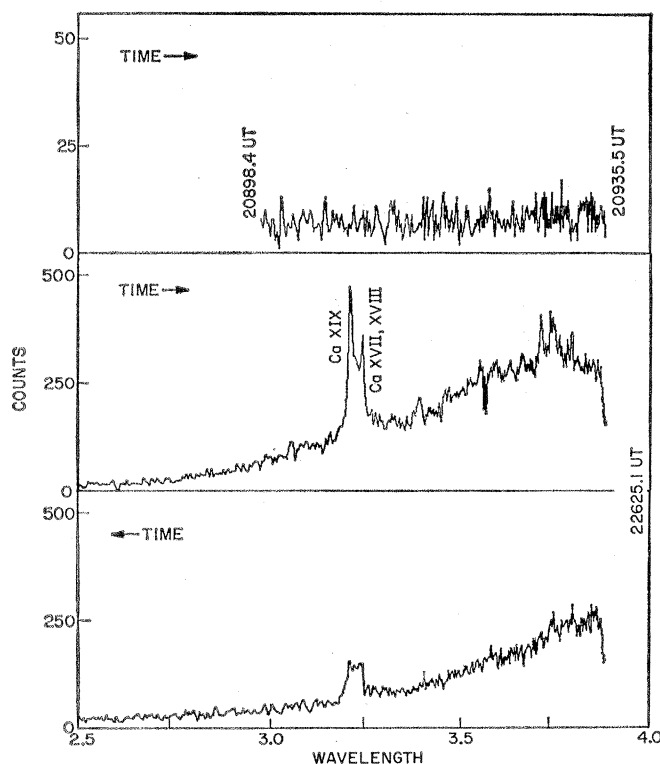


Fig. 6 (left). Uncorrected data derived from the LiF spectrometer for the class 1b flare on 26 October 1967. The vertical scale corresponds to counts per 1.28 second; the horizontal axis is wavelength in angstroms. The top portion of this figure illustrates the solar spectrum before the flare. Universal time is indicated in seconds of the day. Fig. 7 (right). Uncorrected data derived from the EDDT spectrometer for the class 1b flare on 26 October 1967. The vertical scale corresponds to counts per 0.88 second; the horizontal axis is wavelength in angstroms. The top portion of this figure illustrates the solar spectrum before the flare. Universal time is indicated in seconds of the day.

spectrum we have a ratio of roughly 3 : 2, whereas in the later spectrum this ratio is about 1 : 1. The time between measurements is approximately 560 seconds. If we examine the corresponding spectra in Fig. 7, we find that the ratio of Al XII to Mg XI changes from approximately 2 : 1 to 1 : 1; and, while the Si XII has remained roughly the same, Mg XII and Al XIII have both decreased in the same 560 seconds or less. Thus we see that the relative number of higher ionization states decreased with time. Such progressive cooling, evidenced by the ionization distribution, has been inferred from many observations of flare spectra versus time.

Figures 8 and 9 show the raw data from the LiF and EDDT spectrometers, respectively, for the class 3b flare which occurred on 16 November 1967, at about 2125 U.T. Only one complete spectrum is shown for each spectrometer, because there was little or no change from either the preceding or following spectrum scans. During this flare, the spectrometer view direction was moving relative to the flare (that is, the spacecraft's pointed section was executing a raster scan rather than pointing continuously at the center of the sun), so spectrometer position (roughly proportional to θ) has been used as the horizontal axis on both figures. Tape records of raster position versus time will be supplied to us at some later date and will permit conversion of spectrometer position to precise Bragg angle. The vertical axes are the same as in Figs. 6 and 7. Again the instrumental K absorption edges of aluminum and argon are clearly visible. In addition, the silicon absorption edge appears at about 6.7 Å. The increase in continuum at short wavelengths is due to increased reflectivity of the crystals.

The most striking observation is the dominance of continuum emission over line emission in the flare spectrum. In the region below 8 Å, the energy contained in the continuum is one to two orders of magnitude greater than that contained in the lines. With regard to line radiation, the following comments can be made. As shown in Fig. 8, the Ca XIX line is stronger by about a factor of 2 than the K lines of Ca XVII and Ca XVIII. It is also apparent that the profile of the Fe line emission at 1.9 Å is skew, implying that perhaps several lines contribute to the longer wavelength side. Taking into account

the resolution of the crystal, we find that the width of the base of the line is about 15 steps—which is equivalent to 1.5 degrees, which corresponds to 0.075 Å. If the longest wavelength lines in this envelope are the K lines of Fe VII to Fe X at 1.938 Å (3, 4) we find that the shortest lines must be about 1.863 Å, which corresponds closely to the K line of Fe XXIII at 1.865 Å (3).

The small peak at 3.02 Å falls at the position of the Ca XX resonance line (5), but its amplitude is too small to be statistically significant. The peak at position 142 may be K radiation from Ni. No evidence of emission from Fe XXV, 1.86 Å, or Fe XXVI, 1.79 Å, (3, 6, 7) is observed, which is not surprising in view of the low intensity of Ca XX. The behavior of Fe and Ca

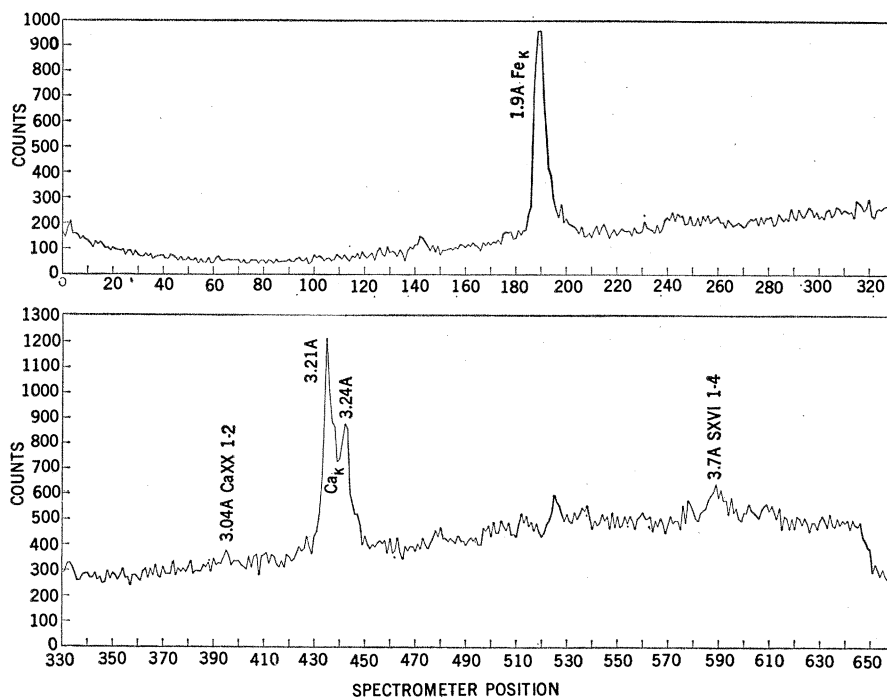


Fig. 8. Uncorrected data derived from the LiF spectrometer for the class 3b flare on 16 November 1967 (2125 U.T.). The vertical scale is counts per 1.28 second. The horizontal axis is spectrometer position in steps of 6 arc min. The line identifications and wavelengths should be considered approximate since θ is changing both because of the spectrometer drive and the motion of the view direction.

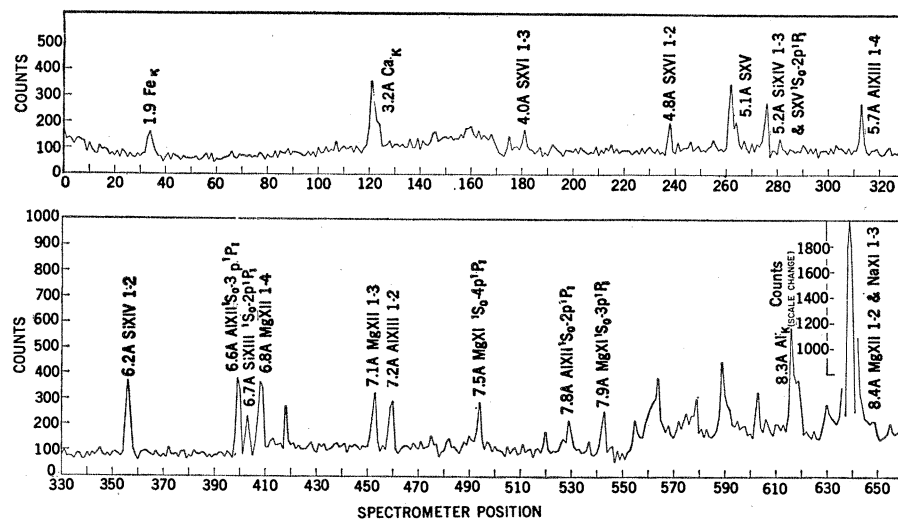


Fig. 9. Uncorrected data derived from the EDDT spectrometer for the class 3b flare on 16 November 1967 (2125 U.T.). The vertical axis is counts per 0.88 second. The horizontal axis is spectrometer position in steps of 6 arc min. The line identifications and wavelengths should be considered approximate since θ is changing both because of the spectrometer drive and the motion of the view direction.

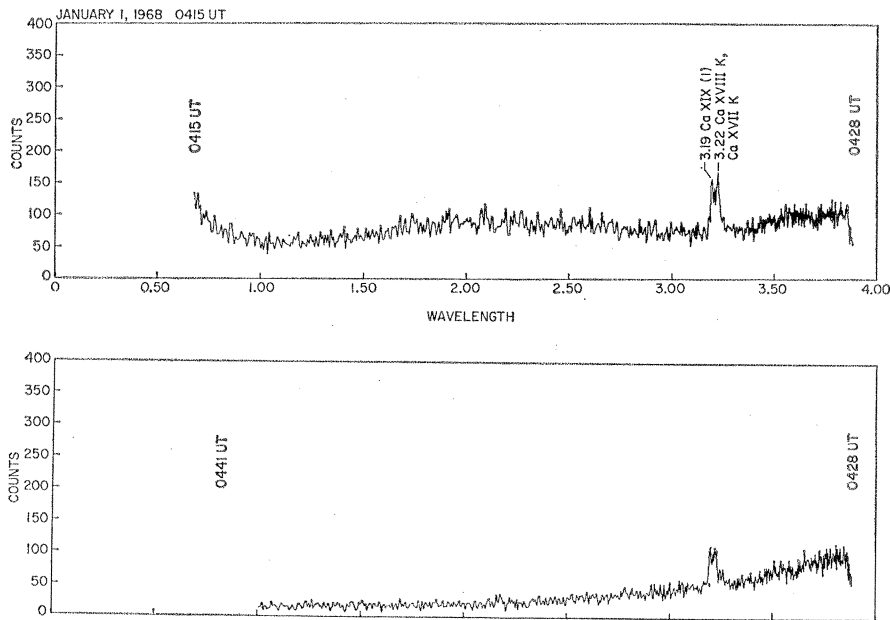


Fig. 10. Uncorrected data derived from two successive wavelength scans of the LiF spectrometer for the x-ray flare on 1 January 1968 (0415 U.T.). The vertical scales are counts per 1.28 second.

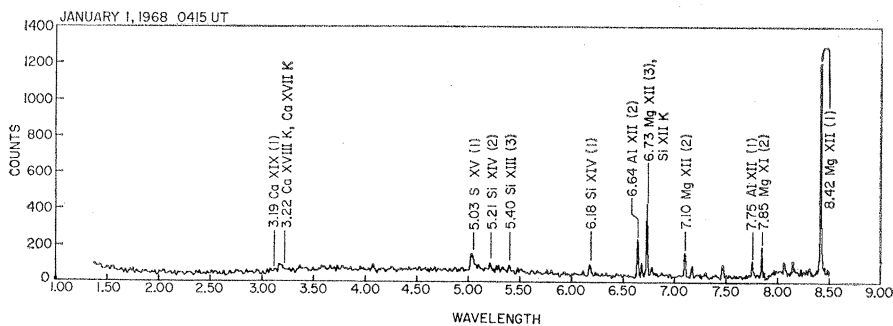


Fig. 11. Uncorrected data derived from the EDDT spectrometer for the x-ray flare on 1 January 1968 (0415 U.T.). The vertical scale is counts per 0.88 second. Only the most prominent lines have been identified in this figure.

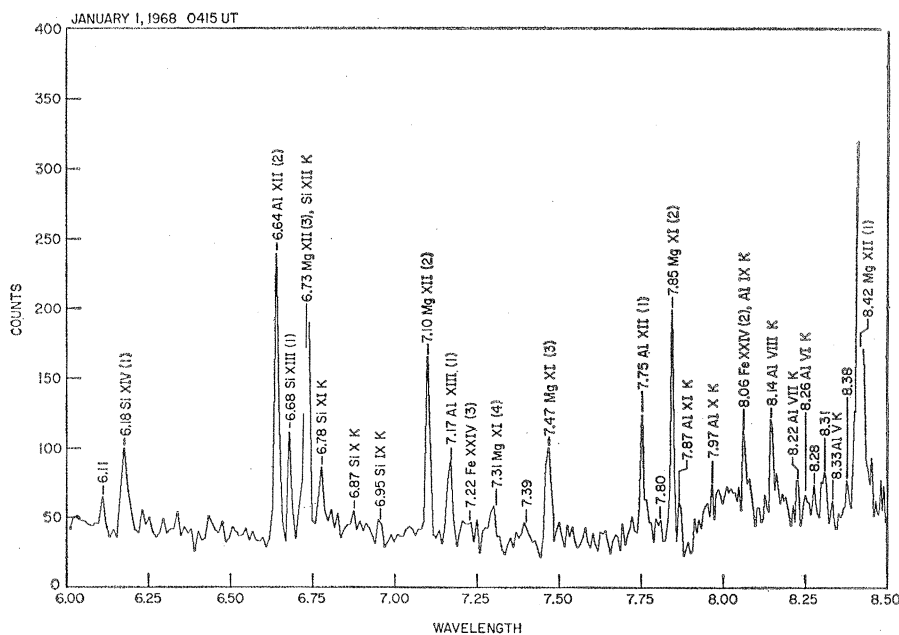


Fig. 12. Expanded 6 to 8.5 Å region of the spectrum of Fig. 11 with identifications.

contrasts with that of S, for which the S XVI resonance emission is almost half that observed from SXV and lesser ionized states. In addition to the labeled lines in Fig. 9, there are the K lines of Al V and Al VII to Al X at 8.3, 8.2, 8.15, 8.1, and 8.0 Å (3), respectively.

The x-ray flare which occurred on 1 January 1968 at about 0415 U.T. gave us an opportunity to determine the wavelengths of solar lines with relatively high accuracy, because the spacecraft instrument was kept in fixed mode, accurately pointed at the center of the sun. Our maximum wavelength error for this event was about 0.005 Å. Figures 10, 11, and 12 are spectra taken of this flare. The K absorption edges of argon, silicon, and aluminum are again obvious. The ratio of continuum to line emission is one to two orders of magnitude during this flare also.

Prominent in Fig. 10 is the feature at 3.2 Å, the lines of Ca XVII, Ca XVIII, and Ca XIX. Iron lines are not present in this spectrum. The continuum shows an increase peaking at about 2 Å. This is due to changes within the flare region with respect to time. The slope of the continuum above 3.3 Å can be used to determine roughly a characteristic temperature, if we assume that all the continuum is bremsstrahlung. The electron temperature so found is 15×10^6 to 20×10^6 °K.

Figure 11 shows the full spectral range of the EDDT crystal with prominent lines identified. The 6 to 8.5 Å region has been expanded and is shown in Fig. 12. Of particular interest are the K lines of Al V to Al XI and Si IX to Si XII, which are present simultaneously with hydrogen-like ions of Al, Mg, and Si. A complete list of the lines which appear in Figs. 10, 11, and 12 is shown in Table 1.

These observations of flare spectra reveal certain characteristics of flare plasma. First, the flare is by no means characterized by an isothermal plasma in thermal equilibrium. For example, in the last flare considered, emission from the lower ionization states of Si and Al would be indicative of ionization equilibrium temperatures in the range of 1×10^6 to 4×10^6 °K, whereas emission from the higher ionization states of the same elements requires temperatures of about 8×10^6 °K. At the same time, the continuum believed to be largely free-free emission, indicates an electron temperature of 15 to 20×10^6 °K. It seems

that we are observing plasmas in which the distribution of ion states departs radically from thermal equilibrium for the local electron temperature, and that a minimum of two parameters, that is, electron temperature and degree of departure from ionization equilibrium as functions of position, must be employed to describe local plasma conditions. This departure from ionization equilibrium is also apparent in the class 3b flare shown in Fig. 8, where continuum slope measurements again indicate electron temperatures of 20×10^6 °K or more, while no appreciable intensity of the helium-like iron and hydrogen-like calcium line emission is produced.

It is interesting to note the absence of the Fe *K*-emission in Fig. 10 at the same time that strong continuum is observed to extend well beyond the *K* critical excitation energy. Although the cross-section for *K* line excitation of Fe is about an order of magnitude less than for the lighter elements Ca, Si, S, and Mg in the 1 to 15 keV range, this factor alone does not appear to be sufficient to explain the absence of the *K* lines of Fe. A quantitative treatment of this problem may provide a mea-

sure of the relative abundance of Fe in the flare region.

The picture of the flare process that may be emerging is one in which rapid local heating of plasma electrons occurs, with energy possibly derived from the self-inductance of a disturbed electrical current system as suggested by Alfvén and Carlqvist (8). The departure from ionization equilibrium may then derive either from the low pressure of the plasma region involved or from the rapidity with which the inductively driven current expands into successive and still "cool" plasma regions, possibly as a result of instabilities which successively choke off the conductivity along each preferred path.

JOHN F. MEEKINS
ROBERT W. KREPLIN
TALBOT A. CHUBB
HERBERT FRIEDMAN

E. O. Hulburt Center for Space Research, Naval Research Laboratory, Washington, D.C. 20390

References and Notes

1. A. Guinier, *X-Ray Diffraction* (Freeman, San Francisco and London, 1963), pp. 100 and 111; R. W. James, *The Optical Principles of the Diffraction of X-Rays* [volume 2 of series, *The Crystalline State*, L. Bragg, Ed. (Cornell Univ. Press, Ithaca, New York, 1965)], pp. 45, 59, 269.
2. B. L. Henke, *J. Appl. Phys.* **26**, 903 (1955); ———, R. L. Elgin, R. E. Lent, R. B. Ledingham, private communication, 1967.
3. L. L. House, preprint submitted to *Astrophys. J.* suppl. (1968).
4. L. W. Acton, *Nature* **207**, 737 (1965).
5. J. D. Garcia and J. E. Mack, *J. Opt. Soc. Amer.* **55**, 654 (1965).
6. L. Cohen, U. Feldman, M. Schwartz, J. M. Underwood, preprint submitted to *J. Opt. Soc. Amer.* (1968).
7. W. M. Neupert, W. Gates, M. Schwartz, R. Young, *Astrophys. J.* **149**, L79 (1967).
8. H. Alfvén and P. Carlqvist, *Solar Phys.* **1**, 220 (1967).
9. H. Flamberg, *Ark. Mat. Astr., Fys.* **28A**, No. 18 (1942).
10. R. L. Blake, private communication.
11. We acknowledge the assistance and cooperation received from personnel of the OSO project office of NASA, Washington, D.C., and from Ball Brothers Research Corporation, Boulder, Colo. From our own support sections at the Naval Research Laboratory, we thank D. E. Simmons, H. W. Smathers, and D. E. Saulnier, who have played key roles in the preparation of the instrument.

27 August 1968

Composition of Aqueous Solutions in Equilibrium with Sulfides and Oxides of Iron at 350°C

Abstract. *Solutions of potassium chloride (pH-buffered and 1-molar) equilibrated at 350°C with pyrrhotite, pyrite, and magnetite contained approximately 1 millimole of reduced sulfur and less than 0.1 millimole of oxidized sulfur per kilogram. Similar solutions equilibrated with pyrite, magnetite, and hematite contained approximately 1 millimole of reduced sulfur, but 3 to 6 millimoles of oxidized sulfur per kilogram. Both types of solutions contained less than 0.1 millimole of iron per kilogram at pH ≥ 6 and approximately 100 millimoles per kilogram at pH 2.*

The oxidation state and concentration of sulfur and of iron in typical hydrothermal solutions from which metallic ores are precipitated have long been debated. We here report on the composition of pH-buffered solutions in equilibrium with the assemblages pyrrhotite (Fe₇S₈ to Fe₉S₁₀)–pyrite (FeS₂)–magnetite (Fe₃O₄) and pyrite–magnetite–hematite (Fe₂O₃). These assemblages were placed in gold capsules with approximately 3 ml of KCl, KCl–HCl–K₂SO₄, or KCl–Na₂S solution, and with either the assemblage potassium feldspar (KAlSi₃O₈)–muscovite [KAl₃Si₃O₁₀(OH)₂]–quartz (SiO₂), or the assemblage muscovite–kaolinite [Al₂Si₂O₅(OH)₄]–quartz. The capsules were flushed with nitrogen, welded shut, placed in a reaction vessel, and held at 350°C under a confining pressure of 270 atm for periods up to 64 days. At the end of each experiment

the reaction was quenched rapidly, the solid phases were x-rayed, and the solution was analyzed.

Runs charged with potassium feldspar, muscovite, and quartz contained only these silicate phases after quenching. On the other hand, most of the runs charged with muscovite, kaolinite, and quartz contained no kaolinite or pyrophyllite [Al₂Si₄O₁₀(OH)₂] detectable by x-ray after quenching. Natural, monoclinic pyrrhotite was used as a starting material. Its composition, as determined by the method of Arnold and Reichen (1), was Fe_{6.95}S₈. At the end of each experiment pyrrhotite had inverted to the hexagonal form with a composition near Fe₉S₁₀, in good agreement with the data of Toulmin and Barton (2). No changes were detected in the x-ray traces of the pyrite, magnetite, and hematite which were used as starting materials.

Table 1. Transitions and wavelengths on 1 January 1968, 0415 U.T.

Ion	Transitions	Wavelength (Å)	Ref.
Al V	<i>K</i>	8.33	(3)
Al VI	<i>K</i>	8.26	(3)
Al VII	<i>K</i>	8.22	(3)
Al VIII	<i>K</i>	8.14	(3)
Al IX	<i>K</i>	8.06	(3)
Al X	<i>K</i>	7.97	(3)
Al XI	<i>K</i>	7.87	(3)
Al XII	1s ² -1s2p	7.75	(3,9,10)
Al XIII	1s-2p	7.17	(5)
Ca XVII	<i>K</i> λ	3.22	(3,10)
Ca XVIII	<i>K</i> ξ	3.22	(3,10)
Fe XXIV	1s ² 2s-1s ² 4p	8.06	(10)
Fe XXIV	1s ² 2s-1s ² 5p	7.22	(10)
Mg XI	1s ² -1s3p	7.85	(9,10)
Mg XI	1s ² -1s4p	7.47	(9,10)
Mg XI	1s ² -1s5p	7.31	(8)
Mg XII	1s-2p	8.42	(5)
Mg XII	1s-3p	7.10	(5)
Mg XII	1s-4p	6.73	(5)
Si IX	<i>K</i>	6.95	(3)
Si X	<i>K</i>	6.87	(3)
Si XI	<i>K</i>	6.81	(3)
Si XII	<i>K</i>	6.73	(3)
Si XIII	1s ² -1s2p	6.68	(3,10)
Si XIII	1s ² -1s3p	5.67	(10)
Si XIII	1s ² -1s4p	5.40	(10)
Si XIV	1s-2p	6.18	(5)
Si XIV	1s-3p	5.21	(5)
Si XIV	1s-4p	4.94	(5)
S XV	1s ² -1s2p	5.04	(3,10)
Unidentified		8.28	
		8.31	